Tannic acid-serum albumin (TASA) complex maintains cell viability and protects from oxidative damage during hypothermic preservation

Dinesh Chaudhary [a, 1], Ines Ferdiana Puspitasari [a, 1], Ju-Yeon Kim [a, 1], Jae-Hyeon Lee [b], Rabyya Kausar [a], Nhu Nam Nguyen [a], Manju Shrestha [a, c], Tien Tiep Nguyen [a], Seho Kweon [d], Simmyung Yook [e, f, *], Taeg Kyu Kwon [g, h, *], Jooho Park [b, *], Jee-Heon Jeong [a, *]

[a]Department of Precision Medicine, School of Medicine, Sungkyunkwan University, Suwon, Gyeonggi 16419, Republic of Korea

[b]Department of Applied Life Science, BK21 Program, Konkuk University, Chungju 27478, Republic of Korea

[c]Research Institute for Convergence Science, Graduate School of Convergence Science and Technology, Seoul National University, Seoul 08826, Republic of Korea

[d]College of Pharmacy, Chonnam National University, Buk-gu, Gwangju 61186, Republic of Korea

[e]School of Pharmacy, Sungkyunkwan University, Suwon, Gyeonggi 16419, Republic of Korea

[f]Department of Biopharmaceutical Convergence, Sungkyunkwan University, Suwon, Gyeonggi 16419, Republic of Korea

[g]Department of Immunology, School of Medicine, Keimyung University, Daegu 42601, Republic of Korea

[h]Center for Forensic Pharmaceutical Science, Keimyung University, Daegu 42601, Republic of Korea

[1]These authors contributed equally to this work.

***Address for correspondence**

Simmyung Yook, Ph.D.

Department of Biopharmaceutical Convergence, School of Pharmacy, Sungkyunkwan University

Suwon, Gyeonggi 16419, Republic of Korea

Phone: +82–31–290–7728; E–mail: ysimmyung@skku.edu

Taeg Kyu Kwon, Ph.D.
Department of Immunology, School of Medicine, Keimyung University
Daegu 42601, Republic of Korea
Phone: +82–53–258–7358; E–mail: kwontk@dsmc.or.kr

Jooho Park, Ph.D.
Department of Applied Life Science, BK21 Program, Konkuk University
Chungju 27478, Republic of Korea
Phone: +82–43–840–3574; E–mail: pkjhdn@kku.ac.kr

Jee-Heon Jeong, Ph.D.
Department of Precision Medicine, School of Medicine, Sungkyunkwan University
Suwon, Gyeonggi 16419, Republic of Korea
Phone: +82–31–299–6165; E–mail: jeeheon@skku.edu

Abstract

Rationale: Clinical translation of mesenchymal stem cell therapies requires preservation methods for maintaining cell viability and function. Preserving mesenchymal stem cells (MSCs) at low temperature represents a clinical approach for maintaining cellular viability during transport and short-term storage of cells intended for therapeutic, diagnostic, and research applications. However, cold-induced stress presents significant challenges in maintaining cell viability and functionality during storage. These challenges underscore the need for strategies to maintain membrane integrity and protect cells from oxidative stress under hypothermic conditions. Here, we developed a hypothermic preservation solution utilizing a combination of tannic acid (TA) and bovine serum albumin (SA), TASA, in basal culture medium.

Methods: MSCs were stored in TASA solutions and evaluated for viability, differentiation capacity, and therapeutic potential. The therapeutic efficacy of TASA-preserved MSCs was assessed further in a dextran sulfate sodium (DSS)-induced colitis mouse model, using disease severity, survival rate, myeloperoxidase activity, gene expression, and histological analysis.

Results: TASA kept MSCs viable *in vitro* for up to 48 h under hypothermic conditions and cleared reactive oxygen species (ROS) better than a commercial preservation solution. TASA-preserved MSCs also retained their therapeutic efficacy in a DSS-induced colitis model, recovering comparably to Fresh MSCs through modulating antioxidant and anti-inflammatory pathways.

Conclusion: TASA maintained MSCs viability and therapeutic function under both *in vitro* and *in vivo* conditions, overcoming cell storage and transport challenges in regenerative medicine.

Keywords: Tannic acid, serum albumin, hypothermic preservation, oxidative stress

Introduction

Cell preservation plays a critical role across healthcare and the food industry [1], particularly in regenerative medicine, where it enables long-term storage of biological products including stem cells, hepatocytes, islets, and CAR-T cells [2]. Hypothermic preservation is the cornerstone of modern biobanking and transplantation, extending the viability of cells, tissues, and organs by reducing metabolic activity and slowing biochemical degradation [3]. Cells under low temperatures show suppressed antioxidant activity, thereby resulting in ROS accumulation, cellular damage, and necrosis, and limiting preservation outcomes [4]. Several hypothermic preservation solutions are now commercially available, including Celsior® (IGL Group, France), Custodiol (Sigma-Aldrich, USA), and Belzer UW (Bridge to Life Ltd., UK) for tissues and organs, and HypoThermosol™ (HTS™; Bio-Life, USA), NutriStor® (Sartorius, Germany), and ROKEPIE-FD01 (Sulfateq BV, Groningen, Netherlands) for cell storage [3, 5]. These formulations have been meticulously designed to maintain ionic and osmotic equilibrium, inhibit acidosis, and prevent cellular swelling during low-temperature storage, thereby enhancing cell viability and function [6]. However, residual toxicity, pH change, limited duration, and insufficient protection during hypothermic preservation remain major challenges in bio-preservation.

Tannic acid (TA) is a natural polyphenol that exhibits strong antioxidant activity by neutralizing ROS and scavenging free radicals [7, 8]. It further enhances cellular defense mechanisms by upregulating antioxidant enzymes such as SOD2 and catalase through activation of the Nrf2 pathway [9]. Previous studies have demonstrated the protective effect of TA against oxidative stress in various cell types. For instance, TA has been shown to protect hepatocytes from acetaminophen-induced oxidative damage and enhance albumin synthesis in these cells [10]. TA has also been shown to attenuate intestinal oxidative damage by improving antioxidant capacity in piglets and intestinal epithelial cells [11]. TA-based nanoparticles have been developed as novel tools to counter oxidative stress, showing ROS-scavenging activity in cells and *in vivo* [12]. However, TA undergoes polymerization and oxidation under various environmental conditions, resulting in degradation and reduced functional activity [13]. Recent studies have reported that serum

albumin (SA) stabilizes TA by forming stable complexes through its colloid-osmotic properties and chaperone-like functions. These SA-polyphenol complexes exhibit enhanced functional properties, including stability, antioxidant activity, and improved protection of biomolecular structures [13-16].

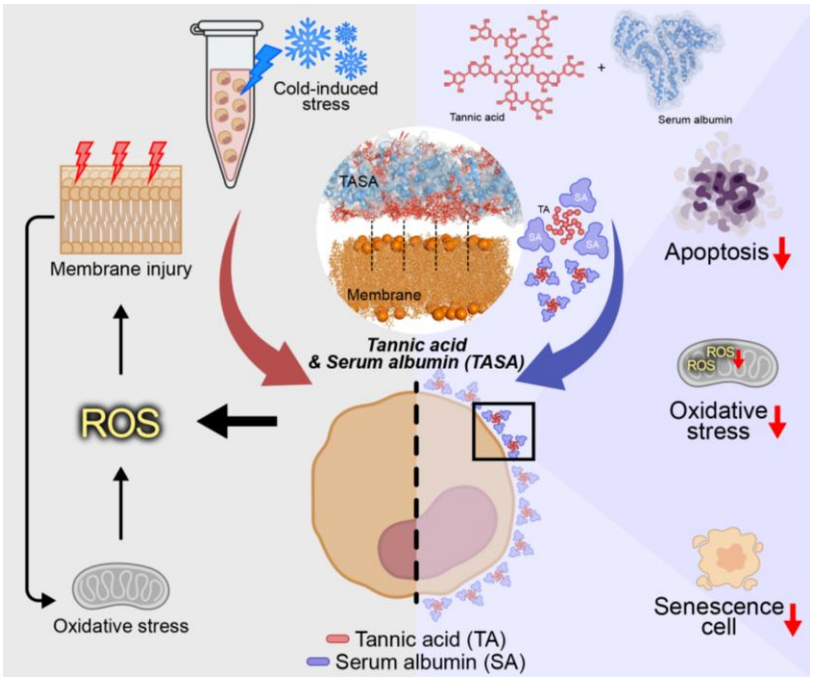

Figure 1. Role of tannic acid-serum albumin (TASA) in hypothermic preservation of cells through modulating oxidative stress.

In this study, we introduced TASA, a tannic acid-serum albumin complex, as a novel hypothermic preservative solution for cells in basal culture media. We demonstrated that the synergistic pairing of TASA strengthened cellular resilience by coupling effective ROS scavenging with enhanced structural integrity in hypothermic preservation. In addition, this study demonstrated that TASA preserves cell viability and metabolic activity, reduces oxidative stress, and promotes multi-lineage differentiation, addressing a key challenge in cell storage and transport for regenerative medicine applications and potentially for clinical use in the future (Figure 1).

Materials and Methods

Animal

Six-to-seven-week C57BL/6 mice (20 ± 2 g) were purchased from Orent Bio (Seongnam, South Korea). The purchased mice were kept at the Laboratory Animal Research Center, Sungkyunkwan University. All animal experiments were approved by the Institutional Animal Care and Use Committee of Sungkyunkwan University (SKKUIACUC2024-07-67-1) and conducted in accordance with the relevant guidelines. Ketamine/xylazine was used to anesthetize mice for collecting serum. Mice were humanely euthanized using CO_2 gas.

Hypothermic preservation of cells

TASA was used to preserve cells in hypothermic conditions. Different concentrations of TA in the TASA complex (SA fixed) and different concentrations of SA in TASA (TA fixed) were used to determine the final optimized conditions of the TASA complex, supplemented with ascorbic acid. Briefly, C57BL/6 mouse adipose-derived mesenchymal stem cells (MSCs) were cultured in DMEM high-glucose medium containing 10% FBS and 1% antibiotics, and incubated in a 5% CO_2 incubator at 37 °C. Once MSCs were confluent, cells were collected and suspended in 1 mL-of basal medium with or without TASA solution and stored at 4 °C for 24, 48, and 72 h. Afterward, cell viability was determined using the live/dead assay and the Cell Counting Kit-8 (CCK-8) assay. As a positive control, Hypothermosol™ (HTS™) was used, which is known to be effective for hypothermic preservation of cells. Additionally, TASA-preserved MSCs were characterized for positive surface markers (CD73 and CD105) and a negative surface marker (CD11b) using flow cytometry [17].

Characterization of TASA complexes

Dynamic light scattering analysis was conducted to confirm complex formation between TA and SA based on size, zeta potential, and polydispersity (PDI) using Zeta Sizer (Nano ZS90, Malvern Instruments, UK).

TA, SA, and TASA solutions were prepared in DMEM and then analyzed. Furthermore, the stability of the TASA complex was evaluated by measuring size, zeta potential, and PDI at days 0, 1, 5, 7, 10, 14, and 21. Additionally, pH and osmolarity were determined in DMEM containing TASA. Moreover, TASA complexes were further characterized using a UV-visible spectrophotometer and fluorescence quenching assay.

In silico analysis of molecular binding

The molecular structure of TA was illustrated using ChemDraw Professional 20.1.1.125 (PerkinElmer Inc.). Docking studies were carried out with AMDock 1.5.2 (Assisted Molecular Docking) against albumin (PDB: 1E7H), employing the CHARMM (Chemistry at Harvard Molecular Mechanics) force field. Before docking, the protein was refined through the Prepare Protein Module in Discovery Studio 2022 (v22.1.0.21297; BIOVIA, California, USA). The binding region was determined from the native ligand site in the PDB structure. During the docking procedure, ten binding poses were generated, and the most energetically favorable pose was selected and visualized with PyMOL (Version 2.1.0; Schrödinger, LLC, NY, USA). Binding affinity values were further calculated to assess the strength of interaction between TA and albumin. To further examine the stability of the TA-SA complex, molecular dynamics (MD) simulations were performed using the Standard Dynamics Cascade protocol in Discovery Studio. The simulations were conducted under an isothermal-isobaric (NPT) ensemble with the generalized distance-dependent dielectric implicit solvent model, running a 5 ns production phase. The resulting simulation trajectories were visualized and analyzed using Discovery Studio software.

Distribution of TASA on the cell surface

To visualize TASA binding to the cell surface, SA was labeled with fluorescein isothiocyanate (FITC) according to the standard conjugation protocol provided by Sigma-Aldrich. SA-FITC was used instead of SA to prepare the TASA-FITC. Briefly, MSCs were incubated with free FITC, SA-FITC, or TASA-FITC,

as in the TASA preservation protocol. Subsequently, MSCs were washed three times with PBS to remove unbound materials, and fluorescence images were taken using a confocal microscope.

Western blot (WB) analysis

Cells and tissues were lysed, and proteins were extracted with RIPA lysis buffer (Sigma-Aldrich, USA) supplemented with protease inhibitors. Protein concentration from each sample was determined using the BCA assay. Briefly, equal amounts of protein were loaded into each well of a 12% SDS-PAGE gel, followed by transfer to a polyvinylidene difluoride (PVDF) membrane (Bio-Rad, USA). Then, the transferred protein membranes were blocked with 5% BSA, followed by incubation with primary antibodies: Bcl-2 (1:1000, Rabbit, BioLegend, USA), Bax (1:1000, Rabbit, Cell Signaling Technology, USA), β-actin (1:1000, Rabbit, Cell Signaling Technology, USA), and secondary antibodies (goat anti-rabbit HRP, Invitrogen, USA) at 4 °C overnight. The next day, the membranes were washed and then incubated with goat anti-rabbit horseradish peroxidase secondary antibody (Invitrogen, USA). β-actin was used as a loading control in WB analysis, while GelQuantNET was used to quantify the protein bands from the blot.

Lipid peroxidation assay

Lipid peroxidation was assessed using a malondialdehyde (MDA) assay kit (MedChemExpress, USA) according to the manufacturer's instructions. Briefly, cells were lysed in RIPA buffer supplemented with 0.5% antioxidant prior to lysis, and protein concentration was determined using the BCA assay. Samples were mixed with MDA detection solution and incubated at 95 ℃ for 30 min to form the MDA-thiobarbituric acid (TBA) adduct. Following centrifugation, the supernatant was transferred to a 96-well plate, and fluorescence was measured at Ex/Em = 515/548 nm using a microplate reader. MDA content was calculated from a standard curve and normalized to protein concentration.

Assessment of cellular fluidity

Cellular fluidity was evaluated using the C-Laurdan probe (MedChemExpress, USA) based on lipid arrangement in the cell membrane. Briefly, cultured MSCs in a 6-well plate were stored at 4 ℃ for 24 h, and then the cells were exposed to the C-Laurdan probe according to the manufacturer's guidelines. Fluorescence was then measured, and the generalized polarization (GP) value was calculated.

Assessment of reactive oxygen species (ROS) scavenging effect

The intracellular ROS-scavenging effect of TASA was determined with the help of 2', 7'-dichlorofluorescin diacetate (DCFDA) assay (Abcam), following the manufacturer's protocols. Briefly, preserved MSCs were washed with PBS and subsequently incubated with 20 μM DCFDA for 30 min. Then, cells were washed with PBS to remove excess dye, and a fluorescence image was taken using a fluorescence microscope (Nikon Eclipse Ti, Japan). For quantitative analysis, the exact number of cells was transferred into black 96-well plates, and fluorescence intensity was measured using a Spark® multimode microplate reader.

Assessment of mitochondrial superoxide and mitochondrial membrane potential

Briefly, MSCs were seeded on a 6-well plate and incubated overnight in a 5% CO2 incubator at 37 °C. Medium from each well was then replaced with DMEM only, HTS™, or TASA, respectively, and the cultured plate was moved to a refrigerator (4 °C) for 24 h. For MitoSOX™ staining, cells were incubated with MitoSOX™ Red reagent (Invitrogen) as per the manufacturer's protocol. For mitochondrial membrane potential, cells were stained with JC-1 dye (Invitrogen), according to the manufacturer's protocol. Fluorescence images were captured and analyzed using a fluorescence microscope (Nikon Eclipse Ti, Japan).

Assessment of cellular senescence

Briefly, 1×10^4 preserved cells per well were seeded in 6-well plates and incubated overnight in a 5% CO_2 incubator at 37 °C. The next day, cells were washed with PBS and fixed using fixative solution from the

senescence β-galactosidase staining kit (Cell Signaling Technology, USA). Then, the fixed cells were incubated in β-galactosidase staining solution prepared according to the manufacturer's protocols. Subsequently, senescent cells were stained with β-galactosidase, and then all images were captured using Optical Microscopy (Nikon Eclipse Ti, Japan).

Assessment of *in vitro* migration study

The wound-healing model was used to evaluate the migration ability of preserved MSCs treated with the TASA solution. Briefly, 3×10^4 preserved cells per well were seeded in 3-well insert plates and cultured until > 95% confluency. Then, cells from the plates were removed, and a narrow, wound-like gap was created, followed by washing with PBS to remove detached cells. Further, the cells were cultured in culture medium for the next 24 h. Then, microscopic images were captured using a fluorescence microscope (Nikon Eclipse Ti, Japan) and further quantified using ImageJ software. For better imaging, the cells were stained with acridine orange (AO).

Assessment of MSCs differentiation

TASA-preserved MSCs were assessed for their osteogenic, adipogenic, and chondrogenic differentiation ability [18]. Briefly, preserved MSCs were cultured in culture medium and exposed to osteogenic, adipogenic, and chondrogenic induction media. Cells were maintained for 21 days, and the media were changed every 3 days. On day 21, the MSCs were stained with Alizarin Red S, Oil Red O, and Alcian Blue to evaluate osteogenic, adipogenic, and chondrogenic differentiation, respectively. Images were captured using Optical microscopy (Nikon Eclipse Ti, Japan).

Assessment of anti-inflammatory activity

Briefly, RAW264.7 cells were seeded in 6-well plates and incubated overnight. Subsequently, RAW264.7 cells were treated with 500 ng/mL of lipopolysaccharide (LPS; Sigma-Aldrich) for 6 h and then co-cultured

with preserved-MSCs (MSC_P) for the next 18 h. Cells were collected and prepared for analysis of inflammatory gene expression via polymerase chain reaction (PCR).

Therapeutic effect of TASA on the colitis mouse model

After one week of acclimatization, C57BL/6 mice were treated with 2% dextran sulfate sodium (DSS) in drinking water (DW) for 5 days [19], followed by dividing into different groups; Control (n = 3, PBS only), PBS (n = 5, DSS + PBS), Fresh MSC (MSC_F; n = 5, DSS + MSC_F), preserved-MSC in DMEM only (MSC_P; n = 5, DSS + MSC_P), 1 h-TASA-treated MSCs (TASA-MSC; n = 5, DSS + TASA-MSC), and TASA-preserved MSCs (TASA-MSC_P; n = 5, DSS + TASA-MSC). On day 5, 2×10^6 cells per mouse were administered intraperitoneally, and the experiments were terminated on day 11. Colons from each mouse were collected and used for colon length measurement, PCR, histology, and myeloperoxidase (MPO) assay. Body weight changes, rectal bleeding, and stool conditions were checked every day before and after treatment with MSCs, which were used for scoring the disease activity index (DAI) [20].

Quantitative real-time polymerase chain reaction (qRT-PCR)

TRIzol (Ambion Life Technology, CA, USA) was used to extract RNA from cells and colon tissues, and RNA quantification was performed using the NanoDrop method (SPARK 10M, TECAN, Austria). Briefly, 1 μg of isolated RNA was used to synthesize complementary DNA (cDNA) using the RevertAid First Standard cDNA Synthesis Kit (Thermo Fisher Scientific). SYBR Green (Thermo Fisher Scientific) was used for qRT-PCR on the QuantStudio real-time PCR system to examine gene expression in cells and colon tissue samples (**Table S1**). *Gapdh* was used as a housekeeping gene for qRT-PCR analysis.

Histological analysis

All feces were removed from the retrieved colon and fixed in 4% formalin for 48 h. Colon tissues were then stored in 30% sucrose solution for the next 24~48 h, followed by sectioning (5 μm) and rehydration. Tissue sections were then soaked in hematoxylin solution for 8 min, and excess stain was washed away with acid

alcohol. Stained tissue sections were incubated in eosin solution, then dehydrated in an ethanol gradient. Furthermore, dehydrated tissue sections were mounted using mounting medium and dried at normal room temperature. Optical images were captured using an optical microscope (Nikon Eclipse Ti, Japan).

In vivo biodistribution study

Briefly, MSCs from different groups: preserved MSCs in DMEM (MSC_P; n = 3), 1 h-TASA-treated MSCs (TASA-MSC; n = 3), and TASA-preserved MSCs (TASA-MSC_P; n = 3) were stored under hypothermic preservation for 24 h and then stained with DiR dye (PerkinElmer, Inc., Waltham, USA), while DiR-stained Fresh MSCs (MSC_F; n = 3) were the control sample. Then, 2×10^6 stained MSCs per mouse were administered through intraperitoneal injection, and their retention was checked at different time intervals (0, 1, and 3 days) using an *in vivo* imaging system (*IVIS*).

Safety evaluation of TASA-preserved MSCs

Fresh MSCs (MSC_F; n = 3)and TASA-preserved MSCs (TASA-MSC_P; n = 3, DSS + TASA-MSC_P) were administered to normal C57BL/6 mice (n = 3), and the serum, bronchoalveolar lavage fluid (BALF), and organs such as the kidney, liver, and lungs were collected after 24 h to assess the biosafety of MSC_F and TASA-MSC_P. Normal C57BL/6 mice without treatment were taken as the control group (Control; n = 3). Serum glutamic pyruvic transaminase (GPT), serum glutamic oxaloacetic transaminase (GOT), and creatinine were measured to assess liver and kidney function, while BALF was used to check the total immune cells. Moreover, the collected organs: kidney, liver, and lungs, were used for histological analysis.

Statistical analysis

All the data were presented as mean ± standard error of the mean (SEM). Statistical analysis was performed using GraphPad Prism V8.4 (GraphPad Software, CA, USA). A one-way analysis of variance (ANOVA) with Tukey's multiple comparisons test was used to assess differences among groups. A p-value of less than 0.05 was considered statistically significant. Moreover, the SRplot was used to generate the heatmap [21].

Results and discussion

Fabrication and characterization of TASA

Although TA is an efficient free radical scavenger, it was essential to optimize its concentration to maximize cell viability; furthermore, SA was employed to stabilize TA. To determine the optimal TASA concentration, different TA and SA ranges were tested for MSC preservation and evaluated by cell viability. Notably, the TASA solution (0.02% TA and 0.05% SA) maintained significantly higher cell viability for over 48 h than the control group (Figure S1A–B). Furthermore, we investigated whether TA or SA alone could maintain cell viability. Neither TA nor SA alone maintained cell viability after 24 h of storage (Figure S1C). However, previous studies have demonstrated that TA maintains cell viability only at high concentrations [22], whereas SA concentrations exceeding 2% have been reported to maintain cell viability during cell storage or transport [22]. These results suggest that SA stabilizes the TA, forming the TASA complex, thereby maintaining cell viability during cold-induced cellular injury during hypothermic storage or transport. Moreover, the pH and osmolarity, as major factors in the culture medium, were analyzed after adding TASA. It seems that the pH and osmolarity of the medium were moderately altered in TASA medium, comparable to free DMEM, indicating its cellular compatibility (Figure S2). Overall, these findings suggest that enhanced hypothermic preservation using TASA is not mainly due to the physicochemical properties of the medium, but rather to its antioxidant and membrane-stabilizing effects.

We performed molecular docking simulations to evaluate interactions between TA and SA, and between TA and cell surfaces. The molecular structure of TA was docked into the SA-binding site (Figure 2A). A 5 ns MD simulation was then performed under an isothermal-isobaric (NPT) ensemble using a generalized distance-dependent dielectric implicit solvent model (Figure 2B). TA remained bound to the three-dimensional structure of albumin without dissociation throughout the simulation. Notably, hydrophobic interactions with several residues, including ASP187, were critical for stable binding, consistent with our previous findings [16, 23]. The TASA interaction network comprised 49-hydrogen bonds, 11-hydrophobic

bonds, and 2 electrostatic interactions (Figure 2C). Van der Waals and interaction energies remained stable with minimal fluctuation throughout the simulations (Figure 2D). Collectively, these results suggested that the TASA complex can be stably formed and maintained under physiological conditions (Figure 2E). To further demonstrate TASA binding to cells, SA was conjugated with FITC to provide a fluorescent signal. Interestingly, a stronger fluorescent signal was observed in the TASA-FITC group compared to the SA-FITC group, indicating stable binding of TASA-FITC on the cell surface (Figure 2F and Figure S3). Similarly, we assessed UV-visible spectroscopy and a fluorescence quenching assay, which confirmed the concentration-dependent interaction between TA and SA (Figure S4A–B) and were consistent with UV-visible spectral changes and fluorescence quenching upon formation of the TASA complex compared to BSA alone [16, 24]. Long-term stability of the TASA complex was analyzed under hypothermic conditions and remained stable throughout the 21 days (Figure S4C). Collectively, these results suggested stable complex formation, which could be applied to protect cells during hypothermic preservation. However, detailed studies of binding stoichiometry and precise molecular structure would be further considered for an in-depth complexation study.

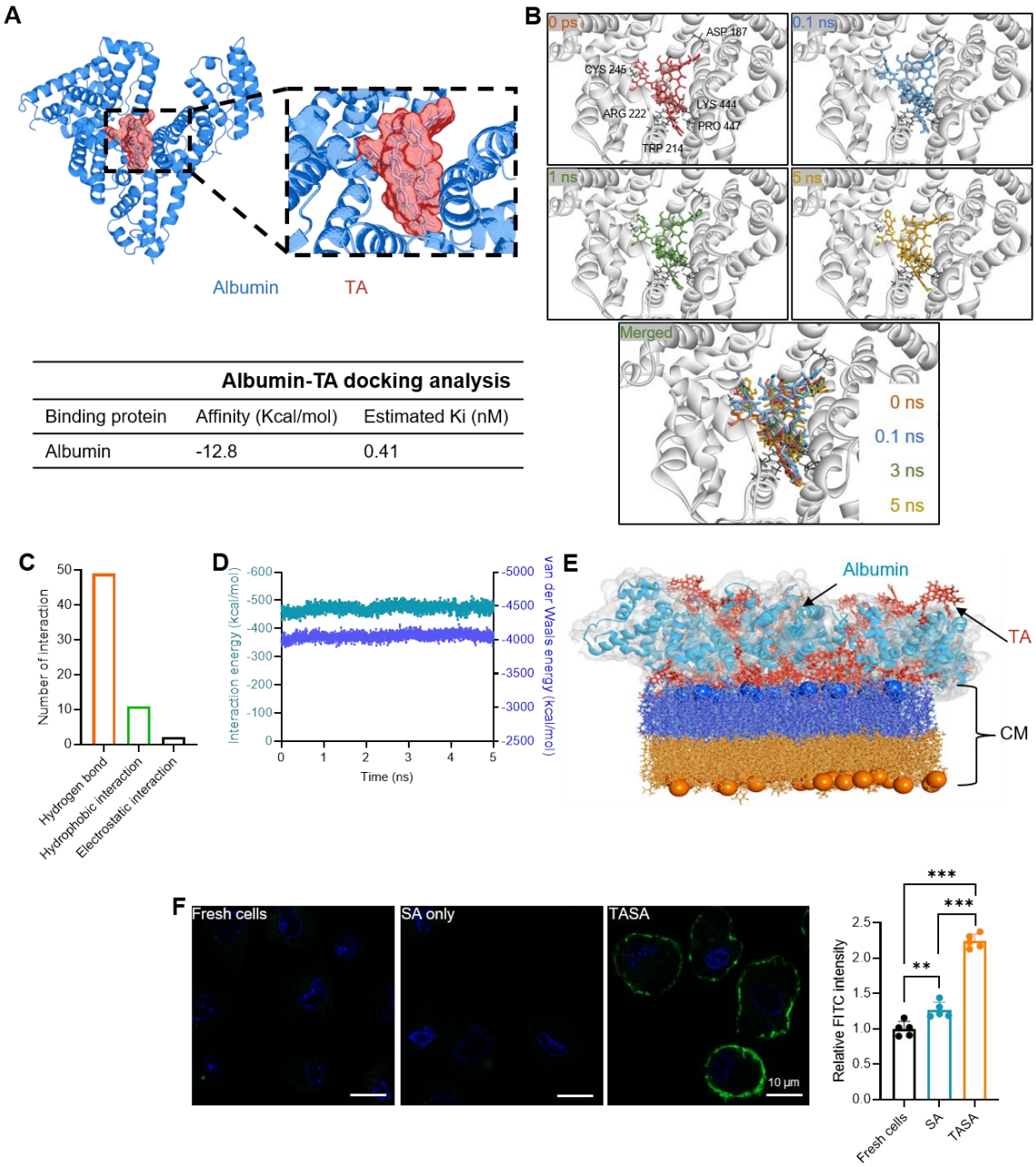

Albumin-TA docking analysis

Binding protein	Affinity (Kcal/mol)	Estimated Ki (nM)
Albumin	-12.8	0.41

Figure 2. Analysis of the interaction between tannic acid (TA) and serum albumin (SA) through molecular dynamics (MD) simulation and fluorescence analysis. (**A**) Docking simulation of TA with albumin, highlighting the binding pocket and docking analysis. (**B**) Representative MD simulation snapshots at 0, 0.1, 1, and 5 ns showing the TA molecule within the albumin binding site, including superimposed trajectories of TA during simulation. (**C**) Classification of major non-bonded interactions observed during the MD simulation. (**D**) Time-dependent profiles of

van der Waals energy and interaction energy during the MD simulation. (**E**) Representative image showing the interaction between TASA and the cell membrane (CM). (**F**) Confocal analysis of mesenchymal stem cells (MSCs) after preserving SA-FITC and TASA-FITC solutions; Hoechst color-stained nuclei, while green color represents the TASA complex (n = 5). Scale bar: 10 μm. Data are expressed as mean ± s.d. A one-way ANOVA with Tukey's multiple comparison test was used for statistical analysis. $^{**}p < 0.01$, and $^{***}p < 0.001$.

Assessment of cell viability on TASA-preserved MSCs

MSCs were stored at 4 °C in three different conditions, DMEM only, TASA, and HTS™, to check their effect on cell viability. CCK-8 assay results showed that TASA maintained cell viability above 70% throughout the 48 h period, which was still higher than that of commercially used HTS™ after 48 h (Figure 3A). However, viability declined across all groups by 72 h, with TASA maintaining significantly higher viability than HTS™ and DMEM only. These results were further confirmed by a live/dead assay, indicating a higher proportion of viable cells in TASA and HTS™ (Figure 3B). During hypothermic preservation, cells undergo stress-induced injury, which significantly affects cell viability. Bax expression showed moderate change across groups, while TASA enhanced Bcl-2 expression (Figure 3C–D and Figure S5–S6). Overall, this analysis demonstrated enhanced survival signaling in TASA-treated MSCs compared to DMEM- and HTS™ preserved cells. A 4 h recovery period allowed time for cell attachment and stabilization. MSCs preserved in TASA rapidly regained function after storage, with adhesion and spreading similar to freshly cultured cells (Figure 3E). This suggested that TASA maintains cell viability and therapeutic function under cold storage, addressing a major challenge in cell transportation.

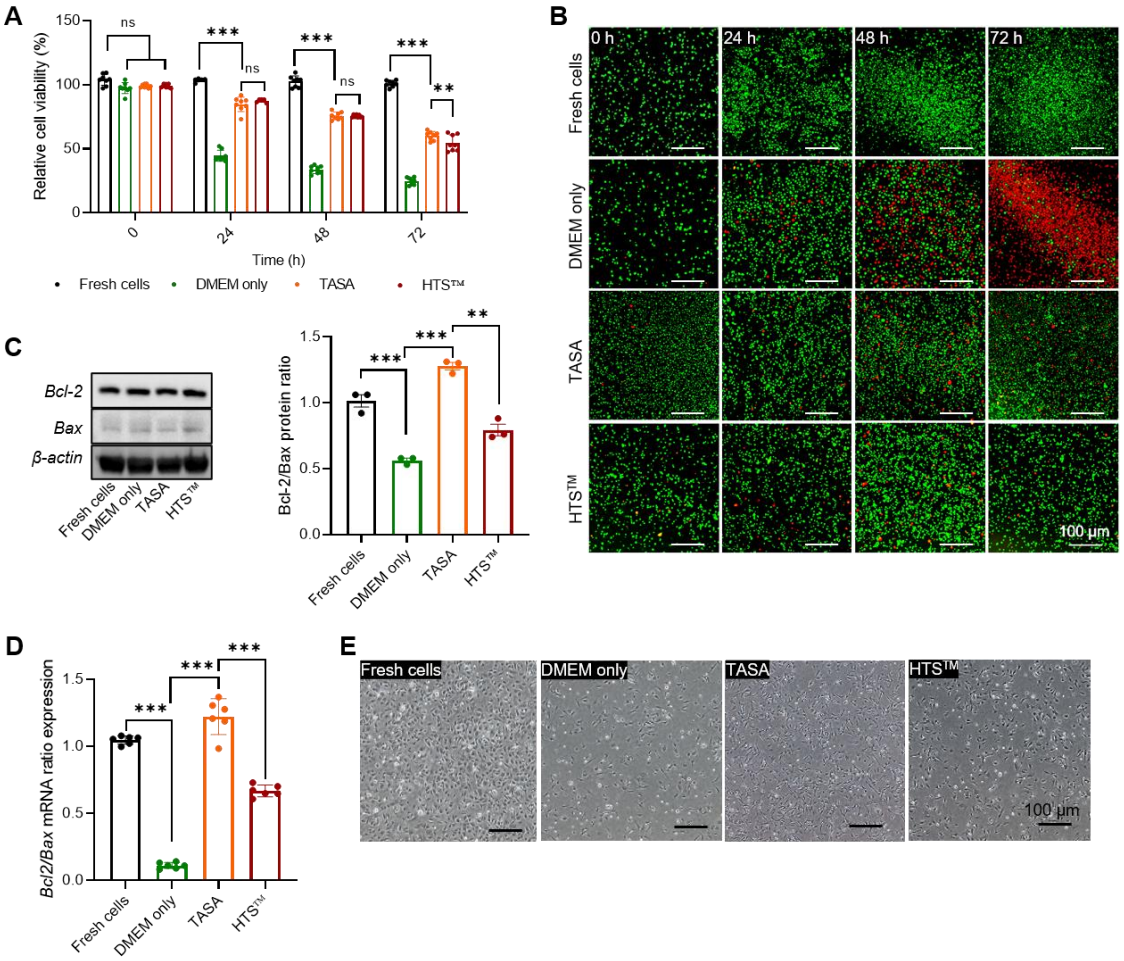

Figure 3. Assessment of cell viability of MSCs after preservation in Tannic acid-Serum albumin (TASA) solution. Cells were suspended in preservation solutions: DMEM only, TASA solution, and HTS™, and stored for 0, 24, 48, and 72 h. Cell viability of MSCs was evaluated in different ways: (**A**) Quantitatively measured using Cell Counting Kit-8 (n = 8); (**B**) Qualitatively determined using a live/dead assay with the help of acridine orange (AO; green fluorescence representing living cells) and propidium iodide (PI; red fluorescence representing dead cells); Scale bar: 100 µm. (**C**) Ratio of Bcl-2 and Bax apoptotic protein levels (n = 3) with their representative protein band and (**D**) mRNA levels (n = 6) determined using Western blot (WB) and qRT-PCR analysis, respectively. β-actin and *Gapdh* were used as a loading control and a housekeeping gene in WB and qRT-PCR analysis, respectively. (**E**) Representative morphology of fresh and preserved MSCs after culture. Scale bar: 100 µm. Data are expressed as mean ± s.d. A one-way ANOVA with Tukey's multiple comparison test was used for statistical analysis. $^{**}p < 0.01$, and $^{***}p < 0.001$; ns, not significant.

Evaluation of intracellular ROS production and senescence on TASA-preserved MSCs

As oxidative stress is a major limitation in hypothermic preservation [3, 4], we further tested the effect of TASA on intracellular ROS production to confirm the maintenance of MSC viability in the TASA solution. Preserved MSCs were treated with hydroperoxide for 24 h to check the intracellular ROS production. Interestingly, MSCs preserved in TASA produce significantly less ROS and exhibit ROS-scavenging activity similar to that of Fresh MSCs. Commercialized HTS™ failed to scavenge ROS, as in DMEM alone and preserved MSC groups (Figure 4A–B). This effect is directly associated with significantly enhanced cellular antioxidant gene expression, including *Sod2*, *Cat*, and *Gpx-1*, in TASA-preserved MSCs compared to other preserved MSCs (Figure 4C–E). These results also confirm that the maintenance of cell viability and functionality in TASA-preserved MSCs reflects the synergistic effect of TA and SA, whereas neither TA nor SA alone preserves MSC viability and functionality. Previous studies have also reported that SA stabilizes TA by forming the TASA complex, reducing its oxidation and prolonging its antioxidant activity [13, 15]. On the other hand, consistent with increased ROS, significantly elevated MDA levels in the DMEM-only group under cold storage conditions indicate peroxidation of membrane phospholipids, resulting in disruption of cell membrane integrity (Figure S7A). However, the TASA group showed an attenuated MDA level, supporting structural integrity of membrane phospholipids comparable to Fresh cells. Beyond the biochemical protection, TASA is expected to confer direct physical protection to the plasma membrane through surface coating, consistent with fluorescence images showing the TASA interaction with the cell surface (Figure 2E–F) as well as with the well-established affinity of hydroxyl groups from tannic acid for forming stable interactions with biomolecular surfaces, independent of its antioxidant activity [25]. In parallel, membrane fluidity assessed by C-Laurdan dye showed increased rigidity under cold storage relative to Fresh cells, and TASA was preserved comparably to HTS™ (Figure S7B–C), supporting a structural, coating-based mode of membrane protection in addition to its antioxidant effect.

As mitochondrial homeostasis is a central determinant of hypothermia-induced cell injury and survival, mitochondrial integrity and dysfunction were evaluated using JC-1 staining and MitoSOX™ staining. Our results demonstrated that DMEM alone under hypothermic conditions could not maintain membrane potential, with a significant reduction compared to Fresh cells ($p < 0.01$), whereas TASA remarkably preserved membrane potential compared with DMEM alone and HTS™, but was comparable to Fresh cells (Figure S8). Consistent with membrane potential, TASA also significantly reduced mitochondrial superoxide accumulation, as indicated by MitoSOX™ fluorescence (Figure S9). These findings support the protective effect of TASA on mitochondrial integrity and oxidative stress in hypothermic-stored cells. While membrane potential is a direct determinant of oxidative ATP synthesis, TASA supports cellular energy metabolism during hypothermic storage. Since cellular ATP levels and energy metabolism have not been studied, further investigations are required to define the effects of TASA on mitochondrial energy metabolism. We evaluated cellular senescence, which is accompanied by increased oxidative stress and a decline in the cellular antioxidant defense system [26-28]. The *p53*, a hallmark of senescence, is activated in response to oxidative stress and DNA damage, which triggers the transcription of *p21*, a cyclin-dependent kinase inhibitor. As the p53/p21 pathway plays a major role in the onset of senescence, p16INK persistently maintains and stabilizes the senescent state of cells [27, 29]. Consistent with this mechanism, MSCs persisted in DMEM only, and HTS™ showed elevated mRNA expression of senescence biomarkers *p21* and *p16*, whereas TASA-preserved MSCs demonstrated a senescence biomarker level similar to that of Fresh MSCs **(**Figure 4F–G), indicating initiation and maintenance of the senescence phase. Likewise, *β*-galactosidase-positive cells were reduced in TASA-preserved MSCs, indicating that TASA effectively suppresses cold-induced cellular senescence (Figure 4H). In summary, TASA upholds cellular antioxidant activity, thereby inhibiting oxidative stress-driven cellular senescence by modulating p53/p21 and p16INK4a pathways.

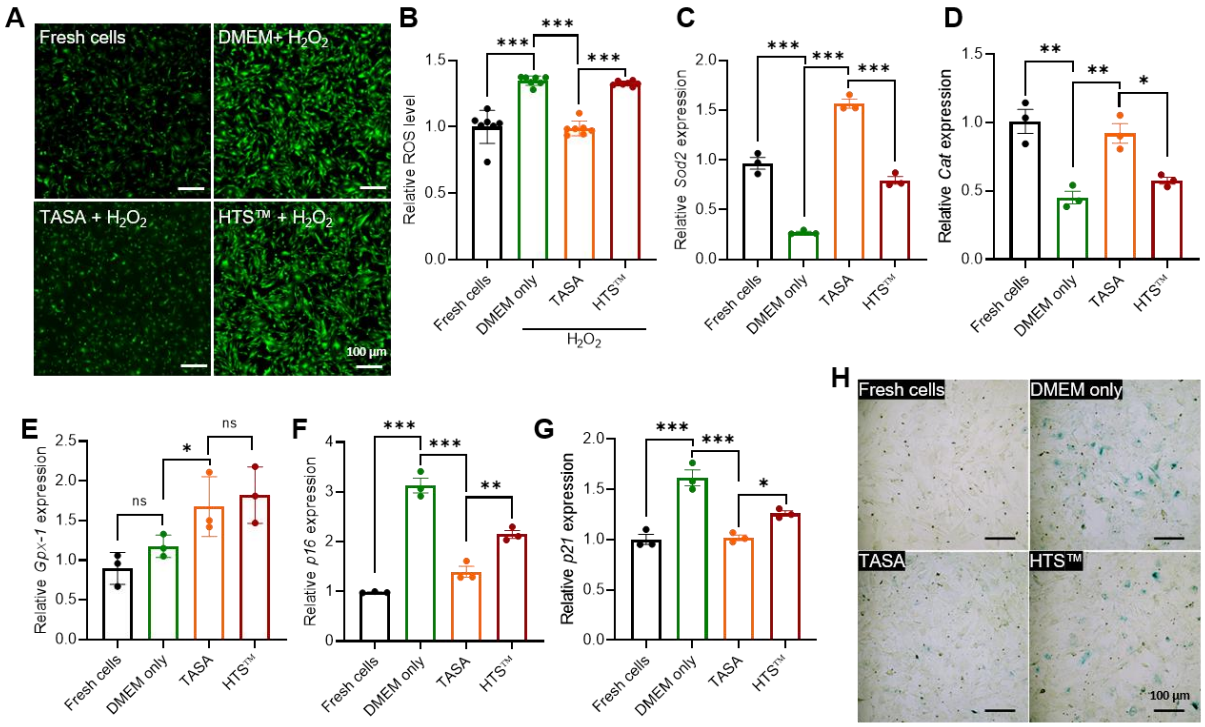

Figure 4. Intracellular reactive oxygen species (ROS) scavenging and the cellular senescence effect of TASA solution after preservation. (**A**–**B**) Representative intracellular ROS as green fluorescence and relative ROS levels using DCFDA analysis (n = 7). Scale bar: 100 μm. (**C**–**E**) The mRNA levels of antioxidant genes: *Sod2*, *Cat*, and *Gpx-1* in preserved MSCs (n = 3). (**F**–**G**) Senescence-associated gene expression: *p16* and *p21* analysis (n = 3). (**H**) Representative images of senescence levels in MSCs using a *β*-galactosidase kit. Scale bar: 100 μm. *Gapdh* was used as a housekeeping gene. Data are expressed as mean ± s.e.m. A one-way ANOVA with Tukey's multiple comparison test was used for statistical analysis. *$p < 0.05$, **$p < 0.01$, and ***$p < 0.001$; ns, not significant.

Assessment of cell migration and multi-lineage differentiation analysis in TASA-preserved MSCs

As MSCs are known for their potential for cell migration and multi-lineage differentiation, as well as their anti-inflammatory properties [28-30], it was necessary to determine whether MSCs retain their functions throughout the TASA preservation process. Therefore, a scratch-wound healing experiment was performed to confirm cell migration. Fresh cells (unpreserved MSCs) with strong wound-closure effects were used as a positive control. Interestingly, TASA-preserved MSCs retained their migratory capacity, demonstrating a

wound-closure rate similar to that of Fresh cells. The TASA group maintained clear superiority over the DMEM-only and HTS™-preserved groups, indicating rapid and effective migration into the scratch area at 12 and 24 h, respectively, and demonstrating that TASA preservation preserves indispensable cellular functions (Figure 5A and Figure S10). In addition to cell migration, multi-lineage staining confirmed the significant preservation of differentiation properties, which have also been used to distinguish MSCs from other cells. TASA-preserved MSCs successfully underwent adipogenic, osteogenic, and chondrogenic differentiation, comparable to Fresh cells (Figure 5B–C). These properties enable MSCs to home to injury sites and contribute to tissue regeneration, making them valuable for cell therapy applications. TASA-preserved MSCs also expressed CD73 and CD105 while lacking CD11b, consistent with standard MSC_F surface markers (Figure S11).

In addition, we tested the anti-inflammatory activity of MSCs, employing a co-culture system with RAW264.7 cells in the presence of LPS (Figure 5D). TASA-preserved MSCs significantly downregulated the expression of pro-inflammatory markers, *Il-6*, *Nf-kβ*, and *Pd-l1*, while the levels of *Il-10* and *Il-22* were well maintained (Figure 5E). Thus, TASA preservation maintains cell viability as well as upholds the functional integrity of MSCs, particularly their anti-inflammatory capacity and multi-lineage differentiation potential.

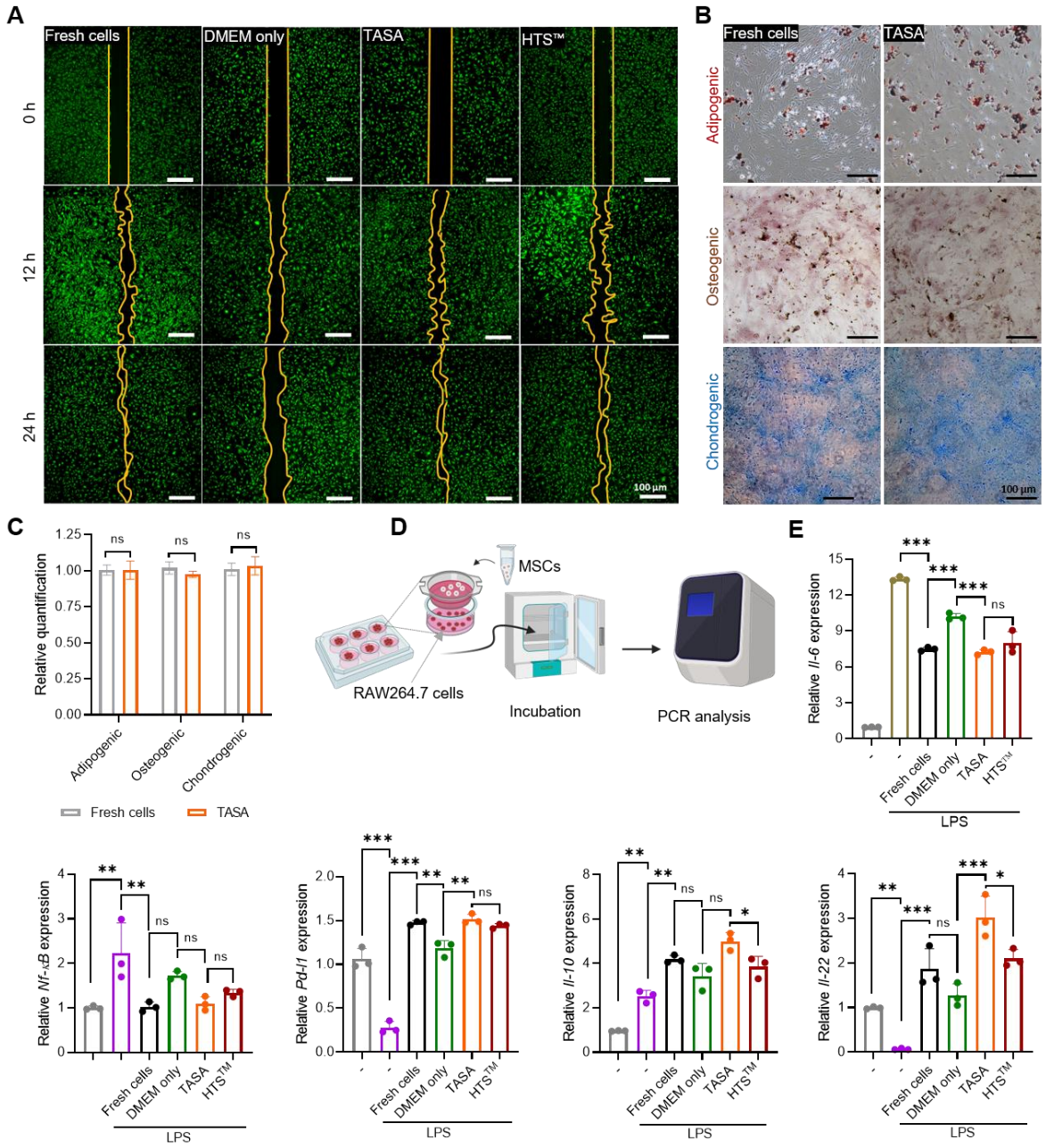

420

421 **Figure 5. Effect of TASA solution on cell migration and differentiation activities of MSCs**. (**A**) Representative
422 image of cell migration using the wound healing model. Scale bar: 100 µm. (**B**) Representative image of MSCs
423 differentiation: Adipogenic (Oil Red O staining), Osteogenic (Alizarin Red S staining), and Chondrogenic (Alcian
424 Blue staining) differentiation. Scale bar: 100 µm. (**C**) Relative quantification of multi-lineage differentiation using
425 ImageJ (n = 3). (**D**) Schematic representation of the methodology for the inflammatory study. (**E**) The mRNA level of

inflammatory-associated gene expression (n = 3). *Gapdh* was used as a housekeeping gene. Data are expressed as mean ± s.d. A one-way ANOVA with Tukey's multiple comparison test was used for statistical analysis. *$p < 0.05$, **$p < 0.01$, and ***$p < 0.001$; ns, not significant.

Therapeutic efficacy of TASA-preserved MSCs in DSS-induced acute colitis model

As the main objective of this study was to preserve MSCs with maintained cell viability and functional integrity, we checked the therapeutic effects of TASA-MSC_P on the DSS-induced acute colitis model to demonstrate the effectiveness of TASA (Figure 6A). DSS-containing drinking water (DW) was given to C57BL/6 mice and withdrawn on day 5, resulting in significant body weight loss. Subsequently, the TASA-MSC_P group showed significant recovery in body weight, comparable to that of the MSC_F group (Figure 6B). DAI also confirmed a remarkable recovery from colitis, although neither group of mice died (Figure 6C–D). Retrieved colons from PBS-treated animals were significantly shortened due to severe inflammation, which typically leads to tissue contraction and a reduction in colon length. Notably, TASA-MSC_P demonstrated significant recovery from colon injury, with colon lengths comparable to those of the control, MSC_F, and TASA-MSC groups (Figure 6E–F and Figure S12). Consistent with the colon length, a remarkable reduction in neutrophil infiltration was confirmed by the MPO assay in colon tissue of the TASA-MSC_P group (Figure 6G). Correspondingly, pro-inflammatory cytokines *Il-6* and *Tnf-α* were downregulated, indicating an overall attenuation in the inflammatory response (Figure 6H). Under DSS treatment, oxidative stress is a major contributor to colon injury, which suppresses or inhibits the Nrf2 antioxidant pathways and plays a key role in maintaining intestinal barrier integrity [30, 31]. Consequently, it causes oxidative damage and impairs cell survival, disrupting intestinal barrier proteins, including occludin, claudins, and zonula occludens-1 [32]. Interestingly, the mRNA expression of *Ocln*, *Zo-1*, *Nrf-2*, and *Vegf* was markedly enhanced in the TASA-MSC_P compared to the PBS and MSC_P groups, reaching levels comparable to those of the control and the MSC groups (Figure 6I). This demonstrates that MSCs activate the antioxidant defense system via *Nrf-2,* which plays a crucial role in reducing oxidative stress

and restoring the intestinal epithelial barrier. In addition, high *Vegf* expression may indicate improved vascular repair and tissue regeneration.

Furthermore, H&E results showed that both the TASA-MSC and TASA-MSC_P groups markedly reduced epithelial damage, immune cell infiltration, and crypt damage in the colon compared with the PBS and MSC_P groups. Similarly, PAS staining showed improved mucus layer integrity, with a high number of goblet cells, thereby protecting and maintaining mucosal homeostasis at the intestinal barrier (Figure 6J). Altogether, the TASA preservative solution demonstrated the preservation of MSCs cell viability and functional integrity, proving the comparable therapeutic potential to MSC_F.

Additionally, we performed *in vivo* cell retention studies in healthy mice for up to 3 days after intraperitoneal administration of DiR-labeled MSCs: MSC_F, MSC_P, TASA-MSC, and TASA-MSC_P. MSC_P group showed a remarkable decline in DiR fluorescence until day 3, indicating poor cell survival after hypothermic preservation (Figure S13). Interestingly, fluorescence from the TASA-MSC and TASA-MSC_P groups was retained on days 0, 1, and 3, comparable to the MSC_F group. It is well known that hypothermic storage of cells triggers ROS accumulation, followed by lipid peroxidation, inflammatory signaling, and cell death before or after transplantation [33, 34]. These results parallel our cell survival and ROS results, which suggest a significant reduction of oxidative stress along with long-term retention in the TASA group, comparable to the Fresh cells group.

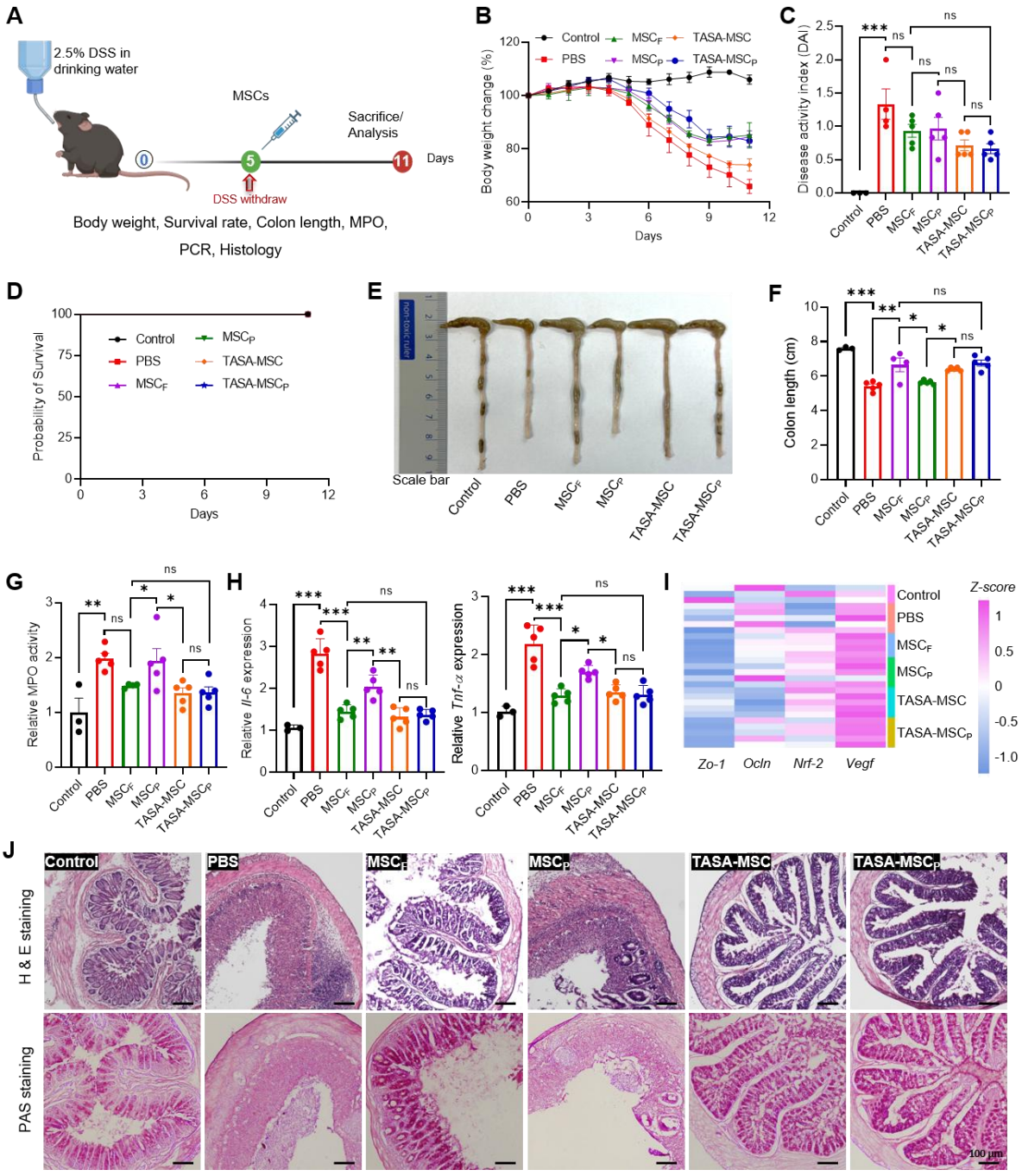

Figure 6. Therapeutic efficacy of preserved MSCs using TASA solution in a dextran sulfate sodium (DSS)-induced colitis mouse model. (**A**) Schematic timeline for study design. (**B**) Body weight change analysis. (**C**) Disease activity index analysis (DAI). (**D**) Survival rate analysis. (**E**–**F**) Representative colon length from different groups and their quantitative analysis after treatment. (**G**) MPO analysis for neutrophil infiltration. (**H**) The mRNA level of inflammatory gene expression in colon tissues. (**I**) Heatmap representing the expression of recovery-related genes

from colon tissues. **(J)** H&E staining and PAS staining of colon tissues. Scale bar: 100 μm. *Gapdh* was used as a housekeeping gene. Data are expressed as mean ± s.e.m. A one-way ANOVA with Tukey's multiple comparison test was used for statistical analysis. *$p < 0.05$, **$p < 0.01$, and ***$p < 0.001$; ns, not significant.

The protein-polyphenol chemistry of TASA may directly stabilize the membrane structure. Albumin within the complex can act as a compliant protein scaffold, while tannic acid provides multivalent crosslinking, thereby reinforcing membrane-associated proteins and lipid packing, analogous to reported tannic acid-mediated supramolecular crosslinking of protein and lipid interfaces that reduces permeability and mechanical fragility [35, 36]. Supramolecular stabilization has been reported to suppress membrane permeability, inhibit lipid peroxidation, and preserve cytoskeletal integrity in polyphenol-coated cells and vesicles, consistent with its role in TASA-treated MSCs. This may explain the maintenance of MSC viability, reduced stress-induced injury, and suppressed intracellular ROS generation following hypothermic preservation, phenomena that closely parallel outcomes in other polyphenol-based cell-coating systems [37, 38]. These effects can persist after removal of the external coating solution; similar transient coatings have been shown to imprint a "protective phenotype" or durable functional shift at the cell surface, despite the noncovalent and reversible nature of the assembly [12, 36].

Conceptually, TASA behaves as a bioinspired, ECM-mimetic interface. The extracellular matrix naturally protects stem cells by providing mechanical buffering, redox regulation, and biochemical signaling; polyphenol–protein supramolecular matrices have been proposed as synthetic analogs that partially recapitulate ECM functions at the cell boundary [39, 40]. TASA recapitulates these roles through a supramolecular, noncovalent, and reversible coating that transiently remodels the MSC surface without genetic modification or permanent chemical alteration, aligning with prior demonstrations of tannic acid-based, cytocompatible surface assemblies on mammalian cells. Therefore, the functional equivalence between TASA-treated and TASA-preserved MSCs supports the interpretation that TASA acts as an autonomous protective coating that integrates physical barrier formation, antioxidant activity, and

membrane-stabilizing protein–polyphenol interactions and is a promising approach for robust stabilization of cells and therapeutic cargo under clinically relevant stress conditions.

Though TASA maintains cell viability and their characteristics, such as multi-lineage differentiation, migration properties, and surface markers, under hypothermic conditions comparable to Fresh MSCs, some limitations need to be addressed for clinical translation. Fresh Cells and TASA-MSC_P did not show remarkable changes in liver markers (GPT and GOT), a renal marker (creatinine), or immune cells in bronchoalveolar lavage fluid (BALF), including H&E staining of liver, lungs, and kidney (Figure S14). Long-term safety evaluation, such as tumorigenicity, genetic stability, and immunogenicity, should be conducted after administration of TASA-preserved MSCs to support comprehensive safety studies before clinical application. As BSA has a xenogeneic origin, this may directly limit clinical translation when used for cell transport. Given that albumin is a stabilizing component in TASA under hypothermic preservation, further investigation will be needed with Xeno-free alternatives or human serum albumin.

Conclusion

We developed TASA, a cell preservative solution, and characterized its ability to maintain cell viability and functional properties such as antioxidant activity, multi-lineage differentiation, migration, and anti-inflammatory activity. MSCs preserved in TASA recovered well after storage and did not undergo cellular senescence. Beyond MSCs, this formulation could be adapted for storing other therapeutic cell types, including hepatocytes, islets, and induced pluripotent stem cells.

Abbreviations

CM: Cell membrane; DCFDA: 2', 7'-dichlorofluorescein diacetate; DSS: Dextran sulfate sodium; MD: molecular dynamics; MPO: Myeloperoxidase; MSCs: Mesenchymal stem cells; PVDF: Polyvinylidene difluoride; ROS: Reactive oxygen species; SA: Serum albumin; TA: Tannic acid; TASA: Tannic acid-serum albumin; TBA: Thiobarbituric acid.

Acknowledgments

This research was supported by the National Research Foundation of Korea (NRF) funded by the Ministry of Science and ICT (grant No. RS-2023-00272815), by the Bio & Medical Technology Development Program of the NRF funded by the Korean government (MSIT) (grant No. 2022M3A9G8017220, RS-2025-02303064, RS-2024-00406114, and RS-2026-25501101) and a Korean Fund for Regenerative Medicine (KFRM) grant funded by the Ministry of Science and ICT and the Ministry of Health and Welfare (grant No. 26B0106L1).

Authors contributions

D.C.: Writing – original draft, Writing – review and editing, Visualization, Validation, Methodology, Investigation, Formal analysis, Data curation, Conceptualization. I.F.P.: Writing – original draft, Visualization, Validation, Methodology, Investigation, Formal analysis, Data curation, Conceptualization. J.-Y.K.: Writing – review and editing, Visualization, Validation, Investigation, Formal analysis, Conceptualization. J.-H.L.: Writing – original draft, Methodology, Investigation, Formal analysis, Data curation. R.K.: Investigation, Formal analysis. N.N.N.: Visualization. M.S.: Visualization. T.T.N.: Visualization. S.K.: Writing – review and editing, Visualization, Formal analysis. S.Y.: Writing – review and editing, Visualization, Validation, Supervision, Project administration, Funding acquisition, Formal analysis. T.K.K.: Writing – review and editing, Visualization, Validation, Supervision, Project administration, Formal analysis. J.P.: Writing – review and editing, Visualization, Validation, Supervision, Project administration, Formal analysis, Conceptualization. J.-H.J.: Writing – review and editing, Visualization, Validation, Supervision, Resources, Project administration, Funding acquisition, Formal analysis, Conceptualization.

Data availability statement

All data for this study are included in the manuscript and supplementary files. Additional data are available upon request to the corresponding author.

Declaration of generative AI and AI-assisted technologies in the writing process

During the preparation of this manuscript, the authors used Grammarly to improve the language and readability. After using this tool/service, the authors reviewed and edited the content as necessary and took full responsibility for the content of the published article.

Competing interests

J.-H.J., S.Y., I.F.P., and S.K. are submitting a patent application that includes work in this manuscript. The authors declare no competing financial interests or potential relationships that could have influenced the work.

References

1. Hanna J., Hubel A. Preservation of stem cells. Organogenesis. 2009; 5: 134-137.

2. Harris DT. Stem cell banking for regenerative and personalized medicine. Biomedicines. 2014; 2: 50-79.

3. Ma Y, Gao L, Tian Y, Chen P, Yang J, Zhang J. Advanced biomaterials in cell preservation: Hypothermic preservation and cryopreservation. Acta Biomater. 2021; 131:97-116.

4. Janssen J, Chirico N, Ainsworth MJ, Cedillo-Servin G, Viola M, Dokter I, et al. Hypothermic and cryogenic preservation of cardiac tissue-engineered constructs. Biomater Sci. 2024; 12: 3866-3881.

5. Freitas-Ribeiro S, Carvalho AF, Costa M, Cerqueira MT, Marques AP, Reis RL, et al. Strategies for the hypothermic preservation of cell sheets of human adipose stem cells. PLOS One. 2019; 16: e0259406.

6. Correia C, Koshkin A, Carido M, Espinha N, Šarić T, Lima PA, et al. Effective hypothermic storage of human pluripotent stem cell-derived cardiomyocytes compatible with global distribution of cells for clinical applications and toxicology testing. Stem Cells Transl Med. 2016; 5: 658-669.

7. Jayachandran B, Parvin TN, Alam MM, Chanda K, Mm M. Insights on chemical crosslinking strategies for proteins. Molecules. 2022; 27: 8124

8. Lou W, Chen Y, Ma H, Liang G, Liu B. Antioxidant and α-amylase inhibitory activities of tannic acid. J Food Sci Technol. 2018; 55: 3640-3646.

9. Sehati F, Ahmadi I, Farivar N, Ranjbaran M, Sadat-Shirazi MS, Nabavizadeh F, et al. Tannic acid protects aged brain against cerebral hypoperfusion via modulation of Nrf2 and inflammatory pathways. Neurosci Lett. 2021; 765: 136263.

10. Lin YH, Lin YC, Hou YT. Prospective application of tannic acid in acetaminophen (APAP)-induced acute liver failure. Int J Mol Sci. 2023; 25: 317.

11. Wang M, Huang H, Wang L, Yin L, Yang H, Chen C, et al. Tannic acid attenuates intestinal oxidative damage by improving antioxidant capacity and intestinal barrier in weaned piglets and IPEC-J2 cells. Front Nutr. 2022; 9: 1012207.

12. Pucci C, Martinelli C, Pasquale DD, Battaglini M, Leo ND, Degl'Innocenti A, et al. Tannic acid–iron complex-based nanoparticles as a novel tool against oxidative stress. ACS Appl Mater Interfaces. 2022; 14: 15927-15941.

13. Zhang F, Tian Y, Fan Z, Liu D, Dai T, Guo Q, et al. In situ engineering mesenchymal stem cells for osteogenic differentiation to reverse inflammaging and restore periodontal bone homeostasis. Adv Funct Mater. 2025:e14199.

14. Raza A, Imran M, Škalko-Basnet N, Obuobi S. Tannic acid-controlled crosslinking of albumin amyloids as multifunctional hydrogels against chronic wounds. Int J Biol Macromol. 2025; 333: 148707.

15. Cometta S, Hutmacher DW. Assessing the biocompatibility of tannic acid-based biomaterials: addressing challenges in standard cytotoxic assays. Bioengineering. 2025; 12: 660.

16. Xu W, Ning Y, Cao S, Wu G, Sun H, Chai L, et al. Insight into the interaction between tannic acid and bovine serum albumin from a spectroscopic and molecular docking perspective. RSC Adv. 2023; 13: 10592-10599.

17. Chaudhary D, Kausar R, Lee JH, Shrestha M, Park JH, Youn YS, et al. Bioengineered hybrid spheroids integrating mesenchymal stem cells and metformin-loaded microspheres for the treatment of sepsis-induced liver injury. J Control Release. 2026; 393: 114798.

18. Ciuffreda MC, Malpasso G, Musarò P, Turco T, Gnecchi M. Protocols for in vitro differentiation of human mesenchymal stem cells into osteogenic, chondrogenic and adipogenic lineages. In: Gnecchi M. Ed. Mesenchymal Stem Cells: Methods and Protocols, 2nd ed. New York: Humana Press; 2016; 1416: 149-158.

19. Kotla NG, Singh R, Baby BV, Rasala S, Rasool J, Hynes SO, et al. Inflammation-specific targeted carriers for local drug delivery to inflammatory bowel disease. Biomaterials. 2022; 281:121364.

595 20. Wirtz S, Neufert C, Weigmann B, Neurath MF. Chemically induced mouse models of intestinal
596 inflammation. Nat Protoc. 2007; 2: 541-546.
597 21. Tang D, Chen M, Huang X, Zhang G, Zeng L, Zhang G, et al. SRplot: a free online platform for data
598 visualization and graphing. PLOS One. 2023; 18: e0294236.
599 22. Shahin H, Elmasry M, Steinvall I, Markland K, Blomberg P, Sjöberg F, et al. Human serum albumin as
600 a clinically accepted cell carrier solution for skin regenerative application. Sci Rep. 2020; 10: 14486.
601 23. Labieniec M, Gabryelak T. Interactions of tannic acid and its derivatives (ellagic and gallic acid) with
602 calf thymus DNA and bovine serum albumin using spectroscopic method. J Photochem Photobiol B. 2006;
603 82: 72-78.
604 24. Xie L, Wehling RL, Ciftci O, Zhang Y. Formation of complexes tannic acid with bovine serum albumin,
605 egg ovalbumin and bovine beta-lactoglobulin. Food Res Int. 2017; 102: 195-202.
606 25. Baldwin A, Booth BW. Biomedical applications of tannic acid. J Biomater Appl. 2022; 36: 1503-1523.
607 26. Faraonio R. Oxidative stress and cell senescence process. Antioxidants. 2022; 11: 1718.
608 27. Pole A, Dimri M, Dimri GP. Oxidative stress, cellular senescence and ageing. AIMS Mol Sci. 2016; 3:
609 300-324.
610 28. Jung M, Cha S, Lee EK. Mitochondrial quantity-quality imbalance in cellular senescence: practical
611 readouts and minimal assay bundles. BMB Rep. 2026; 59:177-186.
612 29. Mijit M, Caracciolo V, Melillo A, Amicarelli F, Giordano A. Role of p53 in the regulation of cellular
613 senescence. Biomolecules. 2020; 10: 420.
614 30. Zhang Y, Cao P, Qin D, Zhao Y, Chen X, Ma P. Anti-inflammatory, anti-colitis, and antioxidant effects
615 of columbianadin against DSS-induced ulcerative colitis in rats via alteration of HO-1/Nrf2 and TLR4-NF-
616 κB signalling pathway. Inflammopharmacology. 2025; 33: 341-352.
617 31. Akanda KMMD, Mehjabin S, Hasan AHMN, Parvez GMM. Role of reactive oxygen species,
618 superoxide dismutases, and inflammation in association with gut microbiota and inflammatory bowel

disease, In: Mishra N, Ashique S, Garg A, Ed. Inflammatory Bowel Disease and Gut Microbiota, 1st ed. New York: Apple Academic Press; 2025; 349-373.

32. Fu M, Wang QW, Liu YR, Chen SJ. The role of the three major intestinal barriers in ulcerative colitis in the elderly. Ageing Res Rev. 2025; 108: 102752.

33. Awad EM, Khan SY, Sokolikova B, Brunner PM, Olcaydu D, Wojta J, et al. Cold induces reactive oxygen species production and activation of the NF-kappa B response in endothelial cells and inflammation *in vivo*. J Thromb Haemost. 2013; 11: 1716-1726.

34. Zieger MAJ, Gupta MP. Endothelial cell preservation at 10ºC minimizes catalytic iron, oxidative stress, and cold-induced injury. Cell Transplant. 2006; 15: 499-510.

35. Son S, Song S, Lee SJ, Min S, Kim SA, Yhee JY, et al. Self-crosslinked human serum albumin nanocarriers for systemic delivery of polymerized siRNA to tumors. Biomaterials. 2013; 34: 9475-9485.

36. Shavandi A, Bekhit AEA, Saeedi P, Izadifar Z, Bekhit AA, Khademhosseini A. Polyphenol uses in biomaterials engineering. Biomaterials. 2018; 167: 91-106.

37. Sozer SC, Egesoy TO, Basol M, Cakan-Akdogan G, Akdogan Y. A simple desolvation method for production of cationic albumin nanoparticles with improved drug loading and cell uptake. J Drug Deliv Sci Technol. 2020; 60: 101931.

38. Lee S, Lee J, Byun H, Kim S, Joo J, Park HH, et al. Evaluation of the anti-oxidative and ROS Scavenging Properties of epigallocatechin gallate (EGCG)-coated biomaterials for tissue engineering. Acta Biomater. 2021; 124: 166-178.

39. Wang XT, Liu LY, Liang H, Ge WY, Chen LL, Jin XQ, et al. Super stable coating based on ovalbumin and tannic acid for hydrophilic and antibacterial functionalization of polymer materials. ACS Appl Mater Interfaces. 2025; 17: 16040-16056.

40. Mogha P, Iyer S, Majumder A. Extracellular matrix protein gelatin provides higher expansion, reduces size heterogeneity, and maintains cell stiffness in a long-term culture of mesenchymal stem cells. Tissue Cell. 2023; 80: 101969.